Hindawi Publishing Corporation
Journal of Sensors
Volume 2015, Article ID 971473, 9 pages
http://dx.doi.org/10.1155/2015/971473

Research Article

Electrophoretic Deposition of SnO_2 Nanoparticles and Its LPG Sensing Characteristics

Göktuğ Günkaya,[1] Mevlüt Gürbüz,[2] and Aydın Doğan[3]

[1]*Department of Ceramics and Glass, Anadolu University, 26470 Eskisehir, Turkey*
[2]*Department of Mechanical Engineering, Ondokuz Mayıs University, 55139 Samsun, Turkey*
[3]*Department of Materials Science and Engineering, Anadolu University, 26555 Eskisehir, Turkey*

Correspondence should be addressed to Göktuğ Günkaya; ggunkaya@anadolu.edu.tr

Received 26 December 2014; Revised 1 April 2015; Accepted 12 April 2015

Academic Editor: Chandra K. Dixit

Homogenized SnO_2 nanoparticles (60 nm) in acetylacetone mediums, both with and without iodine, were deposited onto platinum coated alumina substrate and interdigital electrodes using the electrophoretic deposition (EPD) method for gas sensor applications. Homogeneous and porous film layers were processed and analyzed at various coating times and voltages. The structure of the deposited films was characterized by a scanning electron microscopy (SEM). The gas sensing properties of the SnO_2 films were investigated using liquid petroleum gas (LPG) for various lower explosive limits (LEL). The results showed that porous, crack-free, and homogeneous SnO_2 films were achieved for 5 and 15 sec at 100 and 150 V EPD parameters using an iodine-free acetylacetone based SnO_2 suspension. The optimum sintering for the deposited SnO_2 nanoparticles was observed at 500°C for 5 min. The results showed that the sensitivity of the films was increased with the operating temperature. The coated films with EPD demonstrated a better sensitivity for the 20 LEL LPG concentrations at a 450°C operating temperature. The maximum sensitivity of the SnO_2 sensors at 450°C to 20 LEL LPG was 30.

1. Introduction

The leakage of the LPG, NO_2, SO_2, CO, H_2, and H_2S has a detrimental effect on human health and the environment during production, storage, transportation, and usage stages, due to their toxic and irritating nature [1–3]. Some semiconductor oxides such as TiO_2, ZnO, WO_3, and SnO_2 are the most widely used to detect toxic and explosive gases [4]. SnO_2 is one of the most studied semiconductor oxides among these materials because of its n-type large band gap (3.6 eV) and good quality optical and electrochemical properties [5–8]. SnO_2 is widely used in transparent conducting electrodes, dye-sensitized solar cells, catalytic support materials, high-capacity lithium-storage, electrochemical or photo electrochemical based energy conversions, and gas sensor applications [7–9]. SnO_2 nanoparticles are used for gas sensing applications in particular because of their relatively low operating temperature, simplicity, small dimensions, low cost, high reliability, high surface area, and easy adsorption of oxygen on its surface [10–14]. These properties lead to a high capability in detecting combustible gases such as methane, CH_4, carbon monoxide CO, LPG, and NO_2 [5, 15, 16].

There are various film fabrication technologies that are used to overcome difficulties in sensing applications. Different sensing properties are observed by changing the grain size, film thickness, and porosity of the sensing material. For example, CO and CH_4 can penetrate; hence, both react to the oxygen on the inner SnO_2 grain boundary surfaces. If this was not the case, the other gases such as ethanol, densify on the film surface. The selectivity can be adjusted by controlling the porosity and thickness between the film surface and the electrical contacts [6–8]. A number of coating techniques such as physical vapor deposition (PVD), chemical vapor deposition (CVD), plasma spraying, tape casting, slip casting, thick film screening, and EPD have been published for the deposition of SnO_2 films [17, 18]. EPD has some advantages such as possessing a simple setup, ambient atmosphere operation, and easy control of the composition

and morphologies of the deposited layer when compared to other film deposition techniques [19]. Also, a wide range of thickness from the nanometer to the micrometer scale on curved, rough, or plain (smooth) surfaces is fabricated with EPD. A more uniform and reliable porous ceramic film structure can be easily fabricated by EPD [20]. The EPD technique is based on the movement of the charged particles through the application of an external electric field in the colloidal stable suspension [21]. EPD is defined by two processes: electrophoresis and deposition. Electrophoresis is the migration of the particles under an electric field, whereas deposition refers to the bonding of the moved particles on the desired areas such as the substrate surface and size and size distribution of the ceramic powder, suspension properties, deposition time, and the applied voltage are the main critical parameters to control the film microstructure for EPD [22].

Functional ceramic films such as SiC, ZrO_2, YSZ, ZnO, TiO_2, and SnO_2 have been fabricated with EPD in the field of corrosion resistant layers, electrical insulation, thermal barrier layers, solar cells, sensors, photocatalysts, wear-resistant layers, and optical and structural devices [23–27]. EPD of crack-free magnesium oxide coated SnO_2 films for dye-sensitized solar cells was published by Li et al. Nearly 140 μm of magnesium oxide coated SnO_2 film thickness was successively achieved on FTO glass from colloidal SnO_2 (7 nm) suspension. The photoelectric conversion efficiency above 7% was enhanced for various Mg/Sn ratios [28]. Ui et al. used EPD for lithium secondary batteries using binder-free commercial SnO_2 nanoparticles. They clarified that EPD coated SnO_2 films were effectively operated as the negative electrode for lithium batteries [29]. EPD fabricated SnO_2 films from Sn metal powder for nitrogen dioxide gas detection at low temperatures were reported by Liu et al. They present that the sensing of the sensor to NO_2 gas increased with increasing operating temperature and gas concentration [30]. EPD of the SnO_2 commercial powder to sense CO, O_2, and H_2 gas was published by Gardeshzadeh et al. [31, 32]. They have just concentrated on current-time variations for CO, O_2, and H_2 gas. LPG is the most popular flammable and explosive gas; therefore detection of LPG leakage is extremely important to prevent fatal events and damage to the environment [33]. In literature, the number of studies on the SnO_2 coated surface with the EPD for LPG sensing is quite low.

As stated above, some reports on SnO_2 sensors fabricated with EPD are available to sense LPG. Therefore, the aim of this study is to deposit porous and homogenous SnO_2 films using EPD. Also, the effect of the EPD coating process on the structural, surface morphological, and LPG sensing properties of the SnO_2 films was studied.

2. Experimental Procedure

2.1. Stabilization of SnO_2 Nanoparticles for EPD. In our study, Malvern Nano ZS was used to determine particle size distribution and zeta potential of the SnO_2 solutions using dynamic light scattering. It measures particle size distributions by measuring the angular variation in intensity of light scattered as a laser beam passes through a dispersed and stabile particulate sample. Approximately a 60 nm (17.70 m^2/gr) in average particle size SnO_2 nanopowder was provided from MTI Corp. Two different types of EPD suspensions were prepared in order to compare coating parameters. The first EPD suspension was including iodine (I_2) while in the second one it was without iodine. The first EPD suspension was prepared by mixing SnO_2 with I_2 added acetylacetone (AcAcI). Optimum concentration of the suspension was $50gr_{SnO2}/L_{AcAcI}$. Ultrasonic homogenization was applied to break the agglomerates at 20 watts for 15 minutes. Malvern Nano ZS and sedimentation tests were used to obtain the optimum amount of iodine for stabilization of SnO_2 in acetylacetone (AcAc) and zeta potential measurements. The second EPD suspension was prepared in the same manner in AcAc without iodine. Ultrasonic homogenization at 20 watts for 4 min was applied to disperse the SnO_2 nanoparticles.

2.2. Substrate Preparation and Coating of SnO_2 Using EPD. EPD is a colloidal process based on the motion of charged droplets and particles in a suspension toward an electrode of the opposite charge under an applied DC electric field. Our previous study gives the detailed schematic view of EPD unit. When the electric field is applied to a homogenized suspension surface charged particles migrate toward and away from the charged electrode, and SnO_2 particles accumulate on interdigital electrodes [34]. Figure 1(a) gives the schematic view of interdigital electrode and sensor design. As given in Figures 1(b) and 1(c) sensing element (interdigital electrodes) and heater (back side) were screen printed with Pt paste on the alumina substrates. EPD unit was vertically designed and electrode at the vertical top of the system was used as cathode (coated layer, interdigital electrode). A platinum-palladium (Pt-Pd) sheet was used as counter electrode (anode). Cathode was fabricated Pt coated alumina (Coorstek ADS 996) with 1.2 cm × 1.2 cm surface area. Pt paste for conductive substrate was applied to the surface by brushing, and the second layer was obtained by screen printing. Then, Pt coated alumina substrate was dried in an oven at 130°C for 15 minutes and then sintered at various temperatures for 5, 10, 15, and 20 minutes. At different voltages (50 V–150 V) with various ranges between electrodes (10 mm, 15 mm, and 20 mm) and depositing time (5 sec–120 sec), parameters were experimentally selected for the optimization of the electrophoretic deposition process.

2.3. Sintering and Characterization of EPD Deposited SnO_2 Films. SnO_2 deposited substrates were sintered at a temperature within the range of 300°C and 600°C for 15 minutes in an ambient atmosphere. The film thickness and the microstructures of both the sintered and unsintered SnO_2 layers were examined by a scanning electron microscope (SEM, ZEISS Supra VP 50). The gold-palladium thin film was applied with a sputtering on the top and side surface of the SnO_2 film in order to avoid charging during the SEM characterization.

3. Results and Discussion

3.1. Stabilization of SnO_2 Nanoparticles for EPD. The effect of the various mediums such as acetylacetone, isopropyl

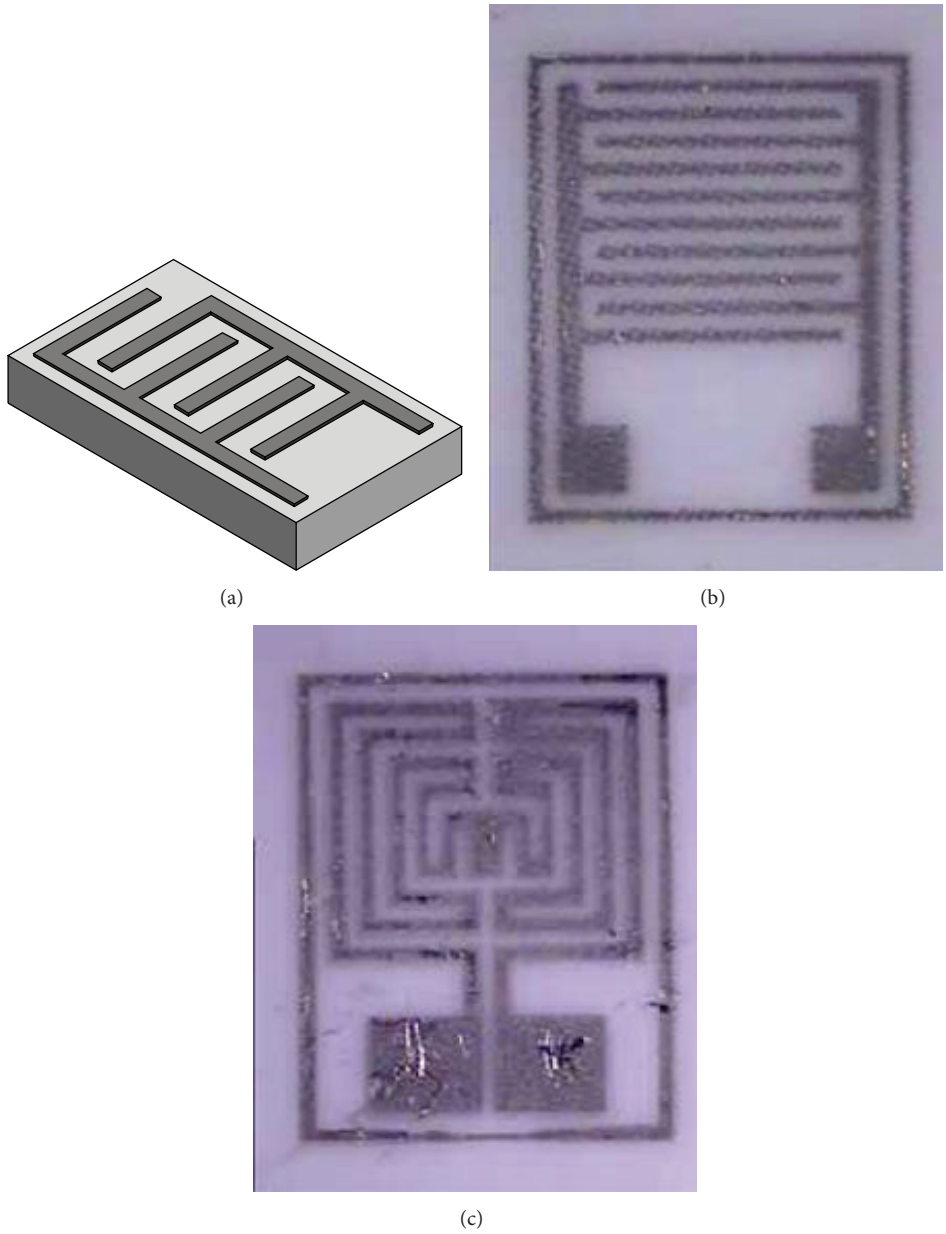

(a) (b) (c)

Figure 1: Schematic view (a), front side (b), and back side (heater) (c) of the sensor.

Table 1: Zeta potential and conductivity of suspensions in three solvent media.

Suspension media	Zeta potential (mV)	Conductivity (μS/cm)
Ethanol	−5.6	0.117
Acetyl acetone	+29	0.00149
Isopropyl alcohol	+55	0.0009

alcohol, and ethanol was experimentally investigated in order to stabilize the SnO_2 nanopowder. Table 1 gives the zeta potential and conductivity of the suspensions. As given in the table, zeta potential and conductivity have a critical role for stabilization and EPD coating. Ethanol has very low zeta potential; therefore the particle is easily precipitated. Isopropyl alcohol has better zeta potential but its conductivity is very poor when compared to other solvents. Therefore migration of the particle is very low. On the other hand acetyl acetone has nearly 30 mV zeta potential and 0,00149 μS/cm conductivity. These values are enough for stabilization and effective EPD coating. The sedimentation tests showed that the best stabilization for the SnO_2 was provided using the acetyl acetone (AcAc) medium. Figure 2 shows the sedimentation test for the SnO_2 particles in both the iodine added and iodine-free AcAc suspension. As shown in Figure 3, the stability of the AcAc based SnO_2 suspension was improved with the iodine addition. The zeta potential value plays a vital role in determining the surface charge of the particles

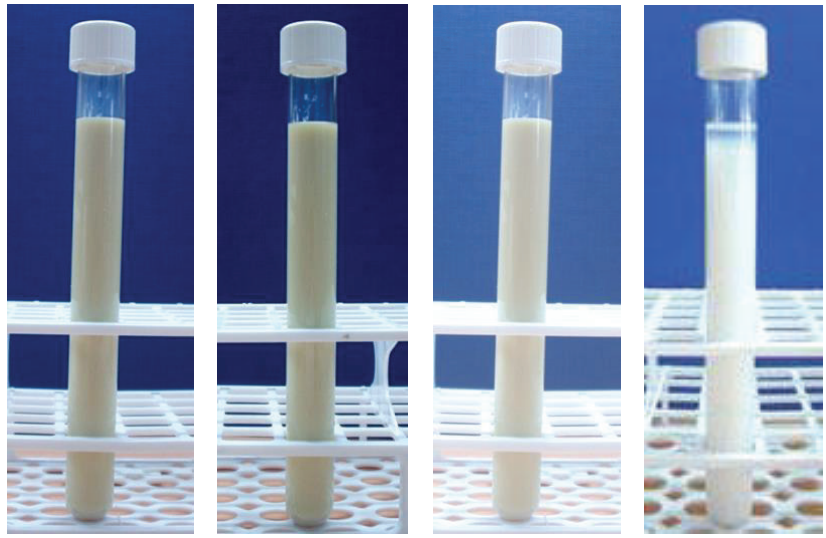

FIGURE 2: Sedimentation test of SnO_2 nanoparticles in iodine added AcAc and AcAc mediums: iodine added AcAc suspension at the beginning of sedimentation test (a), iodine added AcAc suspension after 24 hours (b), suspension without iodine beginning (c), and suspension without iodine after 24 hours (d).

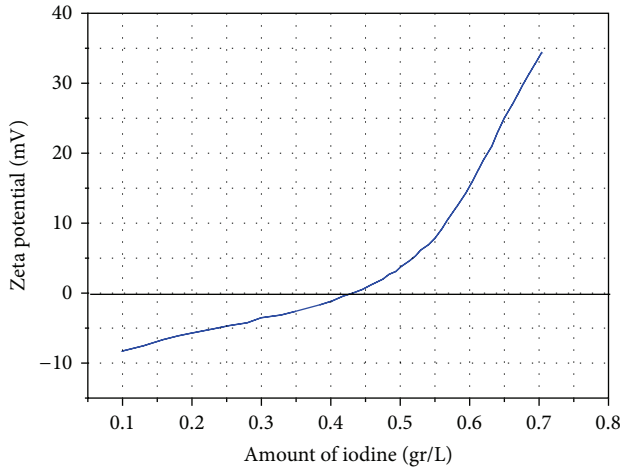

FIGURE 3: Zeta potential of SnO_2 nanopowder in iodine added acetyl acetone medium.

introduced by the zeta potential. Figure 3 shows that zeta potential graph of SnO_2 particles in AcAc based suspension changes from negative to zero up to 0.42 g/L iodine concentration. After this point, it increases zero to positive by changing the amount of iodine. The zeta potential has maximum value (nearly 35 mV) for 0.7 gr/L iodine concentration. Both zeta potential and sedimentation experiments show that stabilization and well-dispersed suspension are achieved by iodine addition. Iodine is used to positively charge the ceramic particles. As given reaction, protons are formed:

$$CH_3COCH_2COCH_3 + 2I_2 \longleftrightarrow ICH_2COCH_2COCH_2I + 2I^- + 2H^+ \quad (1)$$

The iodine reaction between an organic solvent and its alkyls groups creates some ions which is the cause of increasing the suspension conductivity. Therefore, conductivity of acetyl acetone based suspension is much larger than other solvents. This larger conductivity with increasing iodine causes the increase of the zeta potential of ceramic suspension [35, 36].

The evaporation of the iodine from coating layer is a rapid process, but there are still some doubts that it is purified completely. It can cause undesirable reaction and impurity during sensor application. It may act as a contaminant; hence sensor sensitivity or accuracy can change unexpectedly. For this reason, the optimization of the suspension in the absence of iodine is necessary. Because of the probable iodine effect, another suspension was prepared without iodine. The process of the suspension focused on ultrasonic dispersion in this stage. The optimization of the ultrasonic sonification was performed at various times, and power combination was used to enhance the stabilization. The optimum values for the stabilization of the suspension were observed as 20 W and 4 min. The ultrasonic sonification power and time are significant in order to minimize the agglomeration of the particles in the suspension. Excess time and ultrasonic power cause an increase in agglomeration. However, less dispersion time and ultrasonic power combination may cause the insufficient dispersion of the agglomerates. Therefore, the dispersion of the nanosized powder, especially under 100 nm, is very difficult due to the electrostatic attractive forces between the particles [37]. Figures 4(a) and 4(b) show the particle size distribution of the SnO_2 nanopowders. Figure 4(a) displays the trimodel size distribution of suspension prior to the ultrasonic homogenizations process due to agglomeration. However, Figure 4(b) presents the monomodel and the narrow particle size distribution after ultrasonic homogenization. The particle size distribution of

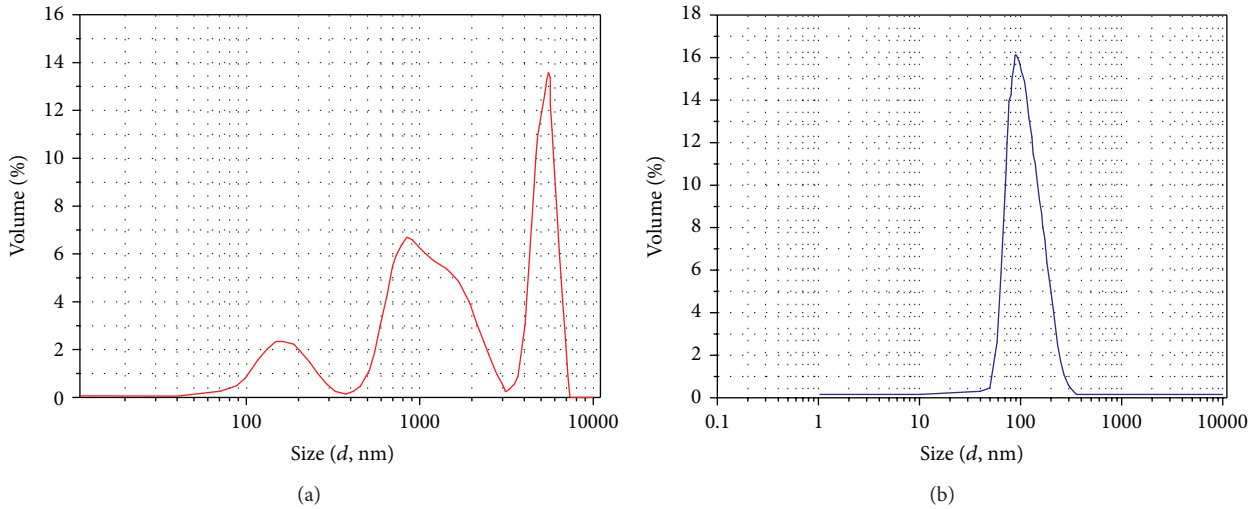

FIGURE 4: Size distribution of SnO_2 nanopowder in AcAc medium before (a) and after optimum ultrasonic homogenization (b).

the SnO_2 in the AcAc without iodine was approximately 100 nm.

3.2. Electrophoretic Deposition of SnO_2 Nanopowder

3.2.1. EPD in Iodine Added AcAc Based SnO_2 Suspension (Process 1). The electrophoretic deposition was performed between 50 and 150 V using AcAcI suspensions. The electrodes' distance and depositing time were 1 cm and 30 sec, 60 sec, 90 sec, and 120 sec, respectively. The optimum deposition voltages were 100 V and 150 V for the SnO_2 accumulation on the interdigital electrodes. The coating quality was adversely affected by either increasing or decreasing the deposition voltage. When the three different deposition voltages were compared, the most homogeneous coating was obtained at 100 V. Figure 5 shows that the migration of the SnO_2 nanopowder at 100 V was higher than the others and resulted in higher deposition yield on any coating surface. Both 50 V and 100 V series have better coating results when compared to 150 V. Migration control of the particles becomes more difficult at higher voltage (150 V). Therefore, suspension concentration between electrodes decreases rapidly, and this causes a decrease in deposition weight.

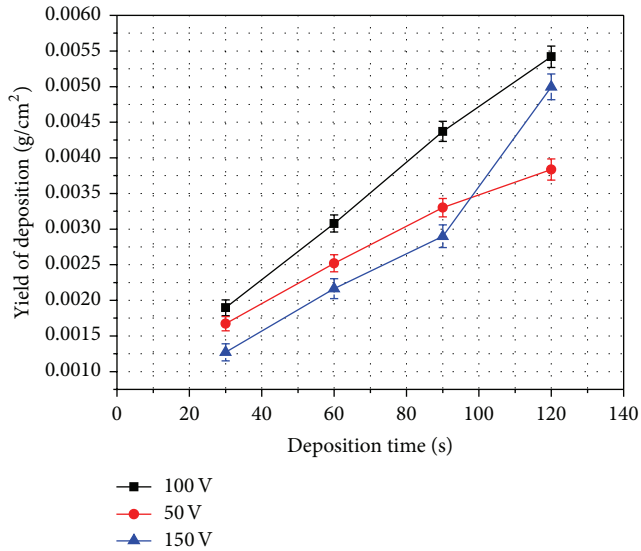

FIGURE 5: EPD of SnO_2 nanoparticles in AcAcI medium at various voltages (50-100-150 V) and deposition time (30-60-90-120 sec).

3.2.2. EPD in AcAc Based SnO_2 Suspension without Iodine (Process 2). The electrophoretic deposition of the SnO_2 nanopowder in the AcAc medium was successfully achieved between 100 and 150 V for a 1 cm electrode distance and various deposition times (5 sec–60 sec). As given in Figure 6, 150 V was the optimum voltage for the SnO_2 deposition when compared to 100 V. As expected, the coating yield increased with deposition time for each coating voltage.

When compared, the EPD of the SnO_2 nanopowder in the AcAc with iodine and the surface charge of the particles in the AcAcI suspension were higher than the AcAc suspension. There was no sedimentation at 24 hours in the AcAcI suspension from the sedimentation test, but nearly 5.4% of the AcAc suspension was precipitated (Figure 2). However, the migration of the SnO_2 particles in the pure AcAc suspension was higher than iodine added suspension even if it has a higher surface charge. It could be explained that the increase of ionic concentration has adverse effect on double layer. Therefore, it causes the reduction of SnO_2 migration during EPD [22]. The weight of EPD coating obtained at 150 V for 30 sec is nearly 0.006 gr/cm^2 (6 times higher than process 1). Therefore, process 2 is more convenient for sensor applications. Also, creating a homogeneous film coating in a short coating time was the main purpose of this study. Therefore, shorter deposition times were investigated for AcAc based suspension. Efficient deposition at 100 V and 150 V for 5 sec and 15 sec produced a homogeneous SnO_2 layer.

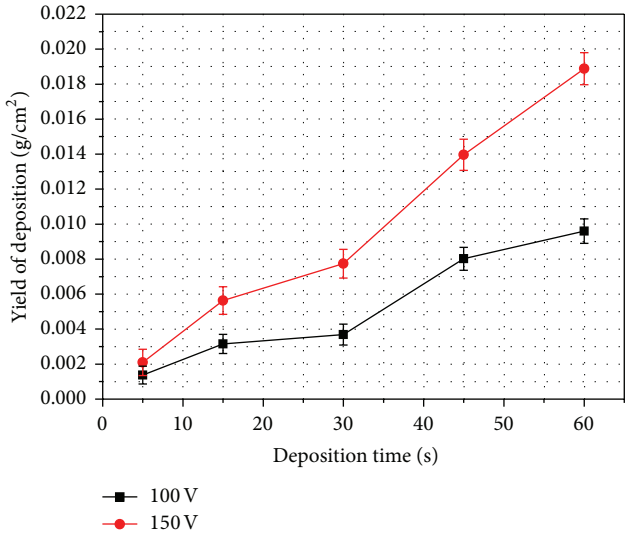

FIGURE 6: EPD of SnO_2 nanoparticles in AcAc medium at various voltages (100-150 V) and deposition time (5-15-30-45-60 sec).

3.2.3. Sintering of Coated SnO_2 Nanopowder with EPD. Porosity, homogeneity, high surface area, and small grain size are the main desired properties of the sensor for increasing the adsorption into certain gases [38]. Because of this reason, a heat treatment should be applied only for the neck formation between the particles in order to enhance the mechanical properties of the deposited layer. Therefore, the microstructure of the deposited SnO_2 films is controllable by the sintering temperature. Nanosized powders possess high surface energy due to their high surface area. The surface energy is the driving force for the sintering. Therefore, nanopowders can be sintered at a low sintering temperature for a shorter sintering time. The sintering temperature range of the SnO_2 commercial powder fluctuates between 1000 and 1400°C, but the nanosized powder is processed at a lower sintering temperature due to its high surface energy [39, 40]. The aim at the sintering step is to determine the neck formation temperature between the SnO_2 nanopowders. The surface diffusion is the dominant sintering (mass transport) mechanism for the SnO_2 within a range of 500–1000°C [39]. Figures 7(a)–7(e) give the sintering behavior of the deposited SnO_2 nanopowders at various temperatures. As the given figure, no neck formation was observed below 500°C (Figures 7(a)–7(c)). The neck formation between the SnO_2 nanopowders was seen at 500°C and 600°C (Figures 7(d) and 7(e)). The SEM investigations showed that the homogeneous SnO_2 film layer was achieved by the EPD on the Pt coated alumina substrate. The film thickness was approximately 6 μm (Figure 7(f)).

3.2.4. Gas Sensing Analyses of the Deposited SnO_2 Films with EPD. Gas sensitivity can be controlled by the surface area and the particle size. The driving force was the high surface area and small pores in the range of the micropore or mesopore in the film structure using the nanopowder in the gas sensing applications. The sensing mechanisms of the gas sensors explained the surface reactions of the semiconducting oxide with hazardous gases. The LPG sensing performance tested the change in the resistance of the SnO_2 film in the presence of the gases. When the sensor was exposed to the toxic and explosive gases, two reactions occurred on the film surface. The first reaction was the oxygen molecules in air which were physisorbed on the surface sites. They were ionized when taking an electron from the conduction band of the semiconductor. Therefore, the resistance of the gas sensors increases. When the semiconductor oxide sensor is exposed to the reducing gases, it reacts with chemisorbed oxygen. Releasing the trapped electron back to the conduction band, it causes a decrease in the resistance of the semiconductor oxide sensor [41, 42]. As given in Figure 7, the diameter of the nanopowders was smaller than 100 nm, and their pores were below 50 nm. These investigations showed that the deposited layers can be used for LPG sensing.

As well as being used as domestic, commercial, and industrial fuel, it also has an area of use in the automobile sector under the name of autogas [43, 44]. The lowest explosive limit (LEL) is the minimum gas concentration that causes combustion in the air in the presence of an ignition source. The gas leakage concentration should not exceed 20% LEL (<3000 ppm) for safety reasons. Liquefied petroleum gas (LPG) was used for gas sensing experiments. The EPD deposited SnO_2 sensors were placed in a cylindrical chamber (≈3 liter). The test chamber was designed to allow the circulation of the air and gas. The gas sensing measurement was performed between 250°C and 450°C for various LEL concentrations. The sensitivity of the SnO_2 films was determined as $S = R_a/R_g$, where R_a was the resistance of the sensor in the presence of air and R_g was the resistance in the presence of the LPG [41, 45]. The resistance measurements were analyzed with the KEITHLEY 2410-C multimeter.

Figures 8(a) and 8(b) present the sensing results of the SnO_2 sensors. Figure 8(a) shows the sensitivity variation of the SnO_2 sensor as a function of the LPG concentration in the range of 10–100 LEL at different operational temperatures, namely, 300, 350, 400, and 450°C. It was observed that the sensitivity of the sensor increases along with the increasing operation temperature for all the LPG gas concentrations. These results follow a similar trend to Majumder et. al's study, which was related to SnO_2/Pd composite films deposited on the Si/SiO_2 substrates with sputtering [46]. The best sensor sensitivity was observed at 450°C for all the LPG concentration. Moreover, the sensor sensitivity to the 20 and 30 LEL LPG sharply increases above the 350°C operation temperature (Figure 8(b)). It could be related to the presence of more stable adsorbed oxygen depending on the heat treatment after the coating.

In our previous studies we have reported that the sensitivity of electrospray deposited (ESD) sensors was between 1.1 and 2.51 for 20 LEL LPG concentration [2]. The sensitivity of sensors produced by EPD at same LPG concentration was between 12 and 30. As a result, the sensitivity of EPD coated SnO_2 sensors was nearly twelve times greater than ESD coated SnO_2 sensors due to their highly porous structure and larger quantity of powder accumulation. According to

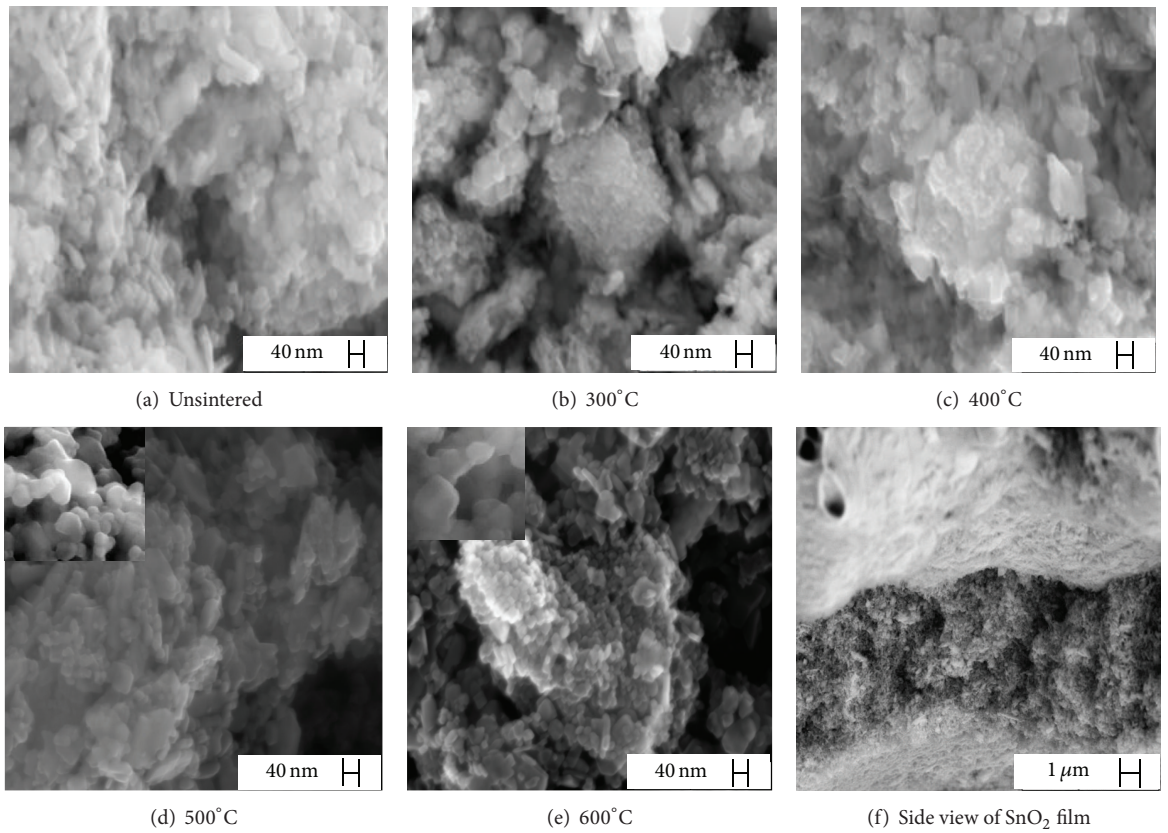

FIGURE 7: SEM images of unsintered SnO_2 (a), sintered SnO_2 at 300°C-400-500-600°C for 5 minutes (b–e), and side view of film thickness (f).

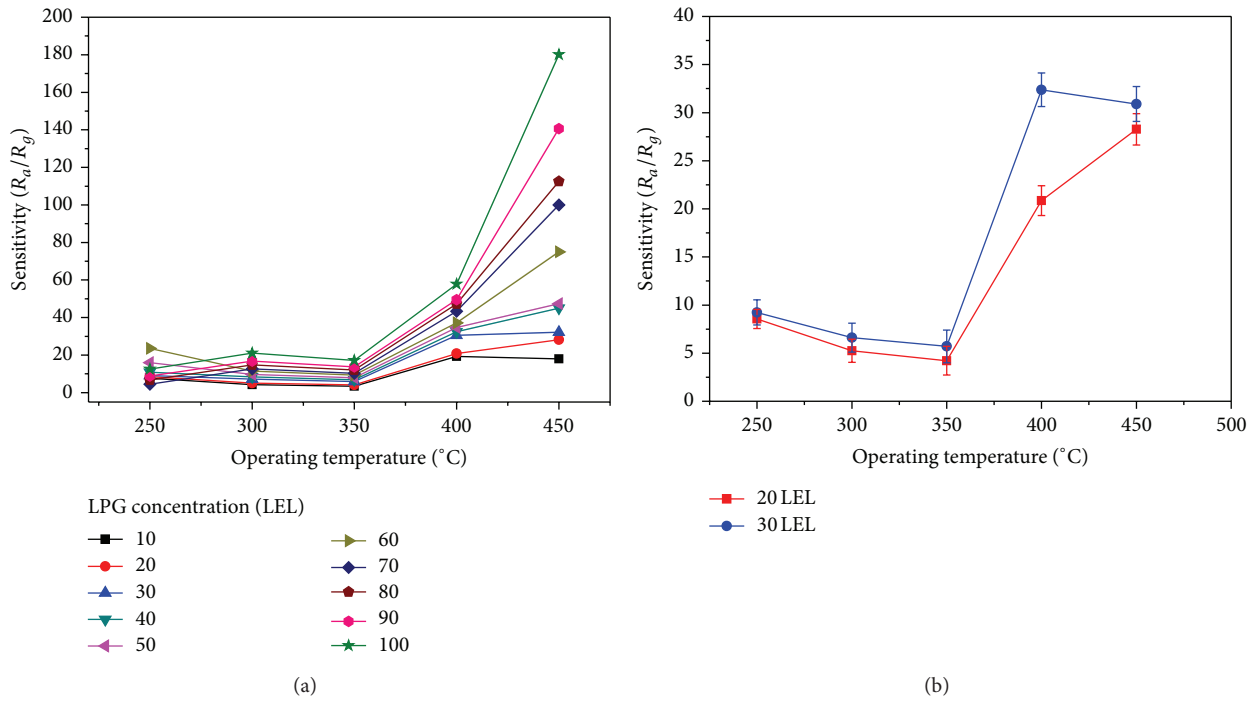

FIGURE 8: Sensitivity of fabricated SnO_2 sensor with EPD: (a) for various LPG concentrations at various operating temperatures and (b) sensitivity to 20 and 30 LEL LPG at various operating temperatures.

our approach, more porous and thicker films can be produced by high deposition voltage, short deposition period, and short distance between electrodes. These were led to increase in the interaction of the particles during migration when the electric field was applied. In this case, individual particles were tended to agglomerate during EPD. These agglomerated particles were created by looser packing and thicker and more porous coating. Consequently, EPD fabricated SnO_2 sensors had higher sensitivity than ESD fabricated sensors.

4. Conclusion

In this study, SnO_2 nanoparticles were effectively deposited into the EPD on Pt coated alumina layer and interdigital electrode. The optimum stabilization of the SnO_2 nanopowder was obtained by dispersing the powders into the acetylacetone medium. The effect of the iodine on the dispersion and deposition of the SnO_2 powders was evaluated. The effective SnO_2 deposition was performed at 100 V and 150 V for 5 sec and 15 sec in the iodine-free AcAc based suspension when the compared iodine was added to the AcAc solution. The sintering of the coating was examined at different temperatures within the range of 300–600°C. The optimum neck formation was achieved at 500°C for 5 min. The coated film thickness was nearly 6 μm. The gas sensing experiments on the LPG were performed for various LPG LEL concentrations. The fabricated sensor with the EPD showed good sensitivity to the 20 LEL LPG at 450°C operating temperature. The best sensitivity of the deposited sensors with EPD at 450°C to 20 LEL LPG was measured at 30.

Conflict of Interests

The authors declare that there is no conflict of interests regarding the publication of this paper.

Acknowledgments

The authors pleased to acknowledge the financial support for this study from Anadolu University, Scientific Researched Project Department, under Grant nos. AUAF040212 and 1404F148. Also, special thanks go to TUBITAK National Young Researcher Career Development Program (104M279) and State Planning Department (DPT 2003K120170) for their financial support.

References

[1] D. Haridas, A. Chowdhuri, K. Sreenivas, and V. Gupta, "Effect of thickness of platinum catalyst clusters on response of SnO_2 thin film sensor for LPG," *Sensors and Actuators B: Chemical*, vol. 153, no. 1, pp. 89–95, 2011.

[2] M. Gürbüz, G. Günkaya, and A. Doğan, "LPG sensing characteristics of electrospray deposited SnO_2 nanoparticles," *Applied Surface Science*, vol. 318, pp. 334–340, 2014.

[3] L. Yang, C. Yin, Z. Zhang, and B. Zhu, "A study of hydrogen sensing properties and microstructure for highly dispersed Pd SnO_2 thin films with high response magnitude," *Applied Surface Science*, vol. 311, pp. 74–82, 2014.

[4] H. Liu, J. Wan, Q. Fu et al., "Tin oxide films for nitrogen dioxide gas detection at low temperatures," *Sensors and Actuators B*, vol. 177, pp. 460–466, 2013.

[5] R. H. R. Castro and D. Gouvêa, "The influence of the Chitosan adsorption on the stability of SnO_2 suspensions," *Journal of the European Ceramic Society*, vol. 23, no. 6, pp. 897–903, 2003.

[6] G. G. Mandayo, E. Castaño, F. J. Gracia, A. Cirera, A. Cornet, and J. R. Morante, "Strategies to enhance the carbon monoxide sensitivity of tin oxide thin films," *Sensors and Actuators B: Chemical*, vol. 95, no. 1–3, pp. 90–96, 2003.

[7] Y. Li, L. Qiao, L. Wang, Y. Zeng, W. Fu, and H. Yang, "Synthesis of self-assembled 3D hollow microspheres of SnO_2 with an enhanced gas sensing performance," *Applied Surface Science*, vol. 285, pp. 130–135, 2013.

[8] S. Das and V. Jayaraman, "SnO_2: a comprehensive review on structures and gas sensors," *Progress in Materials Science*, vol. 66, pp. 112–255, 2014.

[9] X. Lou, C. Peng, X. Wang, and W. Chu, "Gas-sensing properties of nanostructured SnO_2-based sensor synthesized with different methods," *Vacuum*, vol. 81, no. 7, pp. 883–889, 2007.

[10] J. Y. Choi and T. S. Oh, "CO sensitivity of La_2O_3-doped SnO_2 thick film gas sensor," *Thin Solid Films*, vol. 547, pp. 230–234, 2013.

[11] G. D. Khuspe, R. D. Sakhare, S. T. Navale et al., "Nanostructured SnO_2 thin films for NO_2 gas sensing applications," *Ceramics International*, vol. 39, no. 8, pp. 8673–8679, 2013.

[12] B. Esfandyarpour, S. Mohajerzadeh, S. Famini, A. Khodadadi, and E. Asl Soleimani, "High sensitivity Pt-doped SnO_2 gas sensors fabricated using sol-gel solution on micromachined (1 0 0) Si substrates," *Sensors and Actuators B: Chemical*, vol. 100, no. 1-2, pp. 190–194, 2004.

[13] L. Xi, D. Qian, X. Tang, and C. Chen, "High surface area SnO_2 nanoparticles: Synthesis and gas sensing properties," *Materials Chemistry and Physics*, vol. 108, no. 2-3, pp. 232–236, 2008.

[14] H. C. Wang, Y. Li, and M. J. Yang, "Fast response thin film SnO_2 gas sensors operating at room temperature," *Sensors and Actuators B: Chemical*, vol. 119, no. 2, pp. 380–383, 2006.

[15] L. A. Patil, M. D. Shinde, A. R. Bari, V. V. Deo, D. M. Patil, and M. P. Kaushik, "Fe_2O_3 modified thick films of nanostructured SnO_2 powder consisting of hollow microspheres synthesized from pyrolysis of ultrasonically atomized aerosol for LPG sensing," *Sensors and Actuators, B: Chemical*, vol. 155, no. 1, pp. 174–182, 2011.

[16] G. Neri, T. Krishnakumar, R. Jayaprakash et al., "Sb-SnO_2-nanosized-based resistive sensors for NO_2 detection," *Journal of Sensors*, vol. 2009, Article ID 980965, 7 pages, 2009.

[17] C. A. Randall, J. van Tassel, M. Matsko, and C. P. Bowen, "Electric field processing of ferroelectric particulate ceramics and composites," in *Proceedings of the 10th IEEE International Symposium on Applications of Ferroelectrics*, pp. 189–192, IEEE, August 1996.

[18] J. Li, Y. J. Wu, T. Yamamoto, and M. Kuwabara, "Electrophoretic deposition and photoluminescent properties of Eu-doped $BaTiO_3$ thin film from a suspension of monodispersed nanocrystallites," *Science and Technology of Advanced Materials*, vol. 5, no. 4, pp. 393–398, 2004.

[19] M. F. de Riccardis, D. Carbone, and A. Rizzo, "A novel method for preparing and characterizing alcoholic EPD suspensions," *Journal of Colloid and Interface Science*, vol. 307, no. 1, pp. 109–115, 2007.

[20] N. Dougami and T. Takada, "Modification of metal oxide semiconductor gas sensor by electrophoretic deposition," *Sensors and Actuators, B: Chemical*, vol. 93, no. 1–3, pp. 316–320, 2003.

[21] A. Ortona, T. Fend, H.-W. Yu, K. Raju, and D.-H. Yoon, "Fabrication of cylindrical SiCf/Si/SiC-based composite by electrophoretic deposition and liquid silicon infiltration," *Journal of the European Ceramic Society*, vol. 34, no. 5, pp. 1131–1138, 2014.

[22] L. Besra and M. Liu, "A review on fundamentals and applications of electrophoretic deposition (EPD)," *Progress in Materials Science*, vol. 52, no. 1, pp. 1–61, 2007.

[23] K. Raju, H. Yu, J. Park, and D. Yoon, "Fabrication of SiCf/SiC composites by alternating current electrophoretic deposition (AC–EPD) and hot pressing," *Journal of the European Ceramic Society*, vol. 35, no. 2, pp. 503–511, 2015.

[24] E. Caproni, D. Gouvêa, and R. Muccillo, "Yttria-stabilized zirconia closed end tubes prepared by electrophoretic deposition," *Ceramics International*, vol. 37, no. 1, pp. 273–277, 2011.

[25] P. Lommens, D. Van Thourhout, P. F. Smet, D. Poelman, and Z. Hens, "Electrophoretic deposition of ZnO nanoparticles, from micropatterns to substrate coverage," *Nanotechnology*, vol. 19, no. 24, Article ID 245301, 2008.

[26] A. A. Sadeghi, T. Ebadzadeh, B. Raissi, and S. Ghashghaie, "Electrophoretic deposition of TiO_2 nanoparticles in viscous alcoholic media," *Ceramics International*, vol. 39, no. 7, pp. 7433–7438, 2013.

[27] A. R. Gardeshzadeh, B. Raissi, and E. Marzbanrad, "Electrophoretic deposition of SnO_2 nanoparticles using low frequency AC electric fields," *Materials Letters*, vol. 62, no. 10-11, pp. 1697–1699, 2008.

[28] S. Li, Z. Chen, T. Li, Q. Jiang, Y. Wang, and W. Zhang, "Electrophoretic deposition of crack-free magnesium oxide-coated tin oxide film and its application in dye-sensitized solar cells," *Electrochimica Acta*, vol. 133, pp. 275–282, 2014.

[29] K. Ui, S. Kawamura, and N. Kumagai, "Fabrication of binder-free SnO_2 nanoparticle electrode for lithium secondary batteries by electrophoretic deposition method," *Electrochimica Acta*, vol. 76, pp. 383–388, 2012.

[30] H. Liu, J. Wan, Q. Fu et al., "Tin oxide films for nitrogen dioxide gas detection at low temperatures," *Sensors and Actuators, B: Chemical*, vol. 177, pp. 460–466, 2013.

[31] A. R. Gardeshzadeh and B. Raissi, "SnO_2 gas sensor fabricated by low frequency alternating field electrophoretic deposition," *Materials Science in Semiconductor Processing*, vol. 13, no. 3, pp. 151–155, 2010.

[32] A. R. Gardeshzadeh, B. Raissi, E. Marzbanrad, and H. Mohebbi, "Fabrication of resistive CO gas sensor based on SnO_2 nanopowders via low frequency AC electrophoretic deposition," *Journal of Materials Science: Materials in Electronics*, vol. 20, no. 2, pp. 127–131, 2009.

[33] D. S. Dhawale, D. P. Dubal, A. M. More, T. P. Gujar, and C. D. Lokhande, "Room temperature liquefied petroleum gas (LPG) sensor," *Sensors and Actuators B*, vol. 147, no. 2, pp. 488–494, 2010.

[34] A. Dogan, G. Gunkaya, E. Suvaci, and M. Niederberger, "Electrophoretic deposition of nano-sized $BaTiO_3$," *Journal of Materials Science*, vol. 41, no. 24, pp. 8196–8201, 2006.

[35] M. Zunic, L. Chevallier, F. Deganello et al., "Electrophoretic deposition of dense $BaCe_{0.9}Y_{0.1}O_{3-x}$ electrolyte thick-films on Ni-based anodes for intermediate temperature solid oxide fuel cells," *Journal of Power Sources*, vol. 190, no. 2, pp. 417–422, 2009.

[36] H. Maleki-Ghaleh, M. Rekabeslami, M. S. Shakeri et al., "Nanostructured yttria-stabilized zirconia coating by electrophoretic deposition," *Applied Surface Science*, vol. 280, pp. 666–672, 2013.

[37] J. Li, Y. J. Wu, T. Yamamoto, and M. Kuwabara, "Electrophoretic deposition and photoluminescent properties of Eu-doped BaTiO3 thin film from a suspension of monodispersed nanocrystallites," *Science and Technology of Advanced Materials*, vol. 5, no. 4, pp. 393–398, 2004.

[38] S. Basu and P. K. Basu, "Nanocrystalline metal oxides for methane sensors: role of noble metals," *Journal of Sensors*, vol. 2009, Article ID 861968, 20 pages, 2009.

[39] E. R. Leite, J. A. Cerri, E. Longo, J. A. Varela, and C. A. Paskocima, "Sintering of ultrafine undoped SnO_2 powder," *Journal of the European Ceramic Society*, vol. 21, no. 5, pp. 669–675, 2001.

[40] T. Hyodo, N. Nishida, Y. Shimizu, and M. Egashira, "Preparation and gas-sensing properties of thermally stable mesoporous SnO_2," *Sensors and Actuators B: Chemical*, vol. 83, no. 1–3, pp. 209–215, 2002.

[41] A. Srivastava, K. Jain, A. K. Srivastava, and S. T. Lakshmikumar, "Study of structural and microstructural properties of SnO_2 powder for LPG and CNG gas sensors," *Materials Chemistry and Physics*, vol. 97, no. 1, pp. 85–90, 2006.

[42] A. D. Garje and S. N. Sadakale, "LPG sensing properties of platinum doped nanocrystalline SnO_2 based thick films with effect of dipping time and sintering temperature," *Advanced Materials Letters*, vol. 4, no. 1, pp. 58–63, 2013.

[43] D.-S. Lee, D.-D. Lee, S.-W. Ban, M. Lee, and Y. T. Kim, "SnO_2 gas sensing array for combustible and explosive gas leakage recognition," *IEEE Sensors Journal*, vol. 2, no. 3, pp. 140–148, 2002.

[44] S. Chaisitsak, "Nanocrystalline SnO_2:F thin films for liquid petroleum gas sensors," *Sensors*, vol. 11, no. 7, pp. 7127–7140, 2011.

[45] R. S. Niranjan, Y. K. Hwang, D.-K. Kim, S. H. Jhung, J.-S. Chang, and I. S. Mulla, "Nanostructured tin oxide: synthesis and gas-sensing properties," *Materials Chemistry and Physics*, vol. 92, no. 2-3, pp. 384–388, 2005.

[46] S. Majumder, S. Hussain, R. Bhar, and A. K. Pal, "Liquid petroleum gas sensor based on SnO_2/Pd composite films deposited on Si/SiO_2 substrates," *Vacuum*, vol. 81, no. 8, pp. 985–996, 2007.